A Secondary Atomization Model for Liquid Droplet Deformation and Breakup under High Weber Number Conditions

C. A. Chryssakis* and D. N. Assanis
Department of Mechanical Engineering
University of Michigan
Ann Arbor, MI 48109 USA

Abstract

Modern diesel injection systems operate in high injection pressures reaching 210 MPa. The combination of high injection velocities and elevated cylinder pressure results in droplet atomization under high Weber numbers, typically *We*>100, which correspond to the shear and catastrophic breakup regimes. The primary atomization of the liquid jet is modeled using the approach of Huh et al. [6]. The modeling of the secondary atomization is based on a Boundary Layer stripping analysis for the shear atomization regime (80<We<800) and on a combination of Boundary Layer stripping and drop fragmentation analysis for the catastrophic atomization regime (800<We). The drop fragmentation process is predicted from instability considerations on the surface of the liquid drop. A preliminary model evaluation has been performed by comparing the computational results with experimental measurements from isolated drops in shock tube experiments as well as with observations from fully developed diesel sprays.

*Corresponding author: cchryssa@umich.edu

Introduction

Fuel sprays used in internal combustion engines are produced in many different ways, depending on the application and the requirements of each application. There are three basic processes associated with all methods of atomization: the internal flow in the nozzle, the primary and the secondary atomization processes. The spray structure and the characteristics of the spray depend on the internal geometry of the nozzle, the injection pressure and the pressure and temperature conditions in the combustion chamber.

The internal flow in the nozzle can include flow separation and reattachment and to the limit cavitation phenomena that strongly enhance turbulence levels and atomization. Additionally, the design of the nozzle has a major effect on the structure of the spray and its properties. Multi-hole injector nozzles, such as those typically used for diesel applications, result in dense solid-cone jets. The primary atomization of the spray depends on the interaction of the jet structure with the ambient gas, which leads to liquid fragmentation starting with large ligaments close to the core of the jet that further disintegrate into spherical droplets. Once spherical drops are created, after primary atomization has been completed, secondary atomization starts and its governing mechanisms are common for any type of spray [1]. It only depends on the initial droplet sizes, relative velocity between the drop and ambient gas and the physical properties of the system (e.g., pressure, temperature, viscosity, surface tension, etc.). These parameters determine the breakup mechanism under which a droplet will further disintegrate. Even though in a given spray a certain mechanism may be dominant, it is most likely that more than one mechanism will be relevant and they all have to be modeled successfully.

Currently, the atomization process of diesel sprays is commonly modeled using a wave growth or aerodynamic theory that predicts spray parameters such as the spray angle and the drop diameter. The surface wave instability model proposed by Reitz [2], the Kelvin-Helmholtz/Rayleigh-Taylor (KHRT) Instability model by Patterson and Reitz [3] and the Taylor Analogy Breakup (TAB) model by O'Rourke and Amsden [4] are widely used atomization models. However, the coupling with the nozzle effects and the primary atomization is largely unknown and is usually represented by an arbitrary nozzle-dependent constant, which can vary over a factor of 10 for different nozzles [5]. Recently, a model considering both wave growth and turbulence has been developed to provide coupling between the flow inside the nozzle and the exterior atomization process [6]. This model has been adopted here and is briefly described later.

The main objective of this work is to study the physical mechanisms governing secondary atomization, particularly those encountered in diesel engine applications. It has been shown that the physical mechanisms controlling breakup depend on the Weber number of the drops created from primary atomization [1]. The high injection pressures utilized in diesel sprays lead to atomization under high Weber number conditions. Depending on the conditions, the droplets can undergo *shear* or *catastrophic* breakup. The physical mechanisms leading to drop disintegration are described here and they have been represented using a modeling approach that combines a boundary layer stripping assumption in conjunction with a wave instability analysis on the surface of the drop. The new models have been implemented in the three dimensional code KIVA-3V, typically used for internal combustion engine simulations. The model validation has been performed by comparing predictions first with observations of isolated drops and, second, against measurements of typical diesel sprays used in engines.

Primary Atomization

The primary atomization model used in this study is based on the work of Huh, Lee and Koo [6]. The model considers the effects of both infinitesimal wave growth on the jet surface and jet turbulence including cavitation dynamics. Initial perturbations on the jet surface are induced by the turbulent fluctuations in the jet, originating from the shear stress along the nozzle wall and possible cavitation effects. This approach overcomes the inherent difficulty of wave growth models, where the exponential wave growth rate becomes zero at zero perturbation amplitude.

The model is based on two main assumptions:

(i) the length scale of turbulence is the dominant length scale of atomization:

$$L_A = C_1 L_t = C_2 L_w \tag{1}$$

where L_t and L_w are the turbulence length scale and the wavelength of surface perturbations respectively.

(ii) The time scale of atomization is the linear sum of the turbulence and wave growth time scales:

$$\tau_A = C_3 \tau_t + C_4 \tau_w \tag{2}$$

where τ_t is the turbulence time scale and τ_w the wave growth time scale that determines the exponential growth rate. The empirical constants C_1 to C_4 are set to 2.0, 0.5, 1.2 and 0.5 respectively.

The initial turbulence length and time scale are calculated using average quantities for the turbulent kinetic energy and energy dissipation rate. The resulting turbulence length and time scale are given as a function of the time and the initial turbulence conditions as:

$$L_t(t) = L_t^0\left(1 + \frac{0.0828t}{\tau_t^0}\right)^{0.457} \quad (3)$$

$$\tau_t(t) = \tau_t^0 + 0.0828t \quad (4)$$

The wave growth timescale is approximated by neglecting the surface tension and viscous effects and maintaining only the aerodynamic destabilizing term:

$$\tau_w = \frac{L_w}{U}\sqrt{\frac{\rho_L}{\rho_G}} \quad (5)$$

The liquid jet is represented in the form of computational parcels with breakup rate proportional to the ratio of the atomization length and time scale:

$$\frac{dD_p}{dt} = k_1\frac{L_A}{t_A} \quad (6)$$

where the constant k_1 has been set to 0.5. The resulting drop size is assumed to be equal to the atomization length scale, L_A, as calculated with equation (1). When the reduced primary parcel reaches the size of the secondary drop, L_A, the primary atomization process for this parcel is assumed to be completed and the secondary atomization model is engaged.

Drop Deformation and Aerodynamic Drag

In the time period between the end of the primary atomization and prior to secondary breakup the drops deform and reach an ellipsoidal shape, similar to that of an oblate spheroid. Hsiang and Faeth [7] made experiments over a wide range of conditions and concluded that the maximum drop distortion can be given as:

$$\frac{d_{c\max}}{d_o} = 1 + 0.19We^{1/2},\ Oh<0.1,\ We<100 \quad (7)$$

and

$$\frac{d_{c\max}}{d_o} \approx 2,\ Oh<0.1,\ We>100. \quad (8)$$

Assuming linear increase of the drop deformation with time yields:

$$\frac{d_c}{d_o} = 1 + \left(\frac{d_{c\max}}{d_o} - 1\right)\frac{t}{t_{\max}}. \quad (9)$$

According to Aalburg et al. [8], the time required for a drop to reach its maximum deformation is given by:

$$\frac{t_{\max}}{t^*} = 1.53\left(\frac{d_{c\max}}{d_o} - 1\right)^{0.52}, \quad (10)$$

where t^* is a time characteristic, given as:

$$t^* = \frac{d_o}{u_o}\left(\frac{\rho_L}{\rho_g}\right)^{1/2}. \quad (11)$$

The aerodynamic drag forces on a drop can be calculated if the aerodynamic drag coefficient and the cross-sectional area of the drop, normal to the flow, are known. The cross-sectional area can be calculated based on the maximum drop diameter, d_c, since we assume that deformed drops are oblate spheroids. The aerodynamic drag coefficient can be estimated based on the knowledge for drag coefficients for solid bodies of similar shape. According to Clift et al. [9], when a fluid sphere exhibits little internal circulation, either because of high viscosity ratio or because of surface contaminants, the external flow is indistinguishable from that around a solid sphere at the same Reynolds number. Surface contaminants tend to eliminate internal circulation and they exist in most systems of practical importance. Even if bubbles and drops are relatively free of surfactants upon injection, internal circulation decays rapidly as contaminant molecules accumulate at the liquid-gas interface. Considering the fact that the liquid-to-gas viscosity ratio in sprays is high, we can assume that internal circulation is not a significant parameter and rigid-body aerodynamic drag correlations can be used. The deformation of oblate spheroids is described by a single parameter, the aspect ratio, E. The aspect ratio is defined as the ratio of the centerline height to the equatorial diameter of the drop. The final drop deformation, observed when the drop reaches a steady-state condition, is given by:

$$E = \frac{d_{\min}}{d_{\max}} \quad (12)$$

The correlation adopted here (from Clift et al. [9]) for the drag coefficient of a liquid sphere (E=1), is:

$$C_D = \frac{24}{\mathrm{Re}}\left[1 + 0.15\,\mathrm{Re}^{0.687}\right] + \frac{.42}{1 + 4.25\,\mathrm{Re}^{-1.16}\cdot 10^4},\quad Re<3\times10^5. \quad (13)$$

For liquid disks, $E\rightarrow 0$, one can use

$$C_D = \frac{64}{\pi\,\mathrm{Re}}\left(1 + 0.138\,\mathrm{Re}^{0.792}\right),\ 1.5<Re<133 \quad (14)$$

$$C_D=1.17,\ Re>133 \tag{15}$$

For oblate spheroids with aspect ratio E=0.5, Clift et al. suggest:

$$C_D = 108.42\,\mathrm{Re}^{\left(-1.66+.3958\log \mathrm{Re}-0.03\log^2 \mathrm{Re}\right)},\ 40<Re<10^4. \tag{16}$$

The three equations describing drag for the sphere, the disk and the spheroid are plotted in Figure 1. For intermediate values of the aspect ratio, E, linear interpolation will be used in the model. The Reynolds number in the correlations for the disk and the spheroid is based on the cross-sectional diameter, d_c.

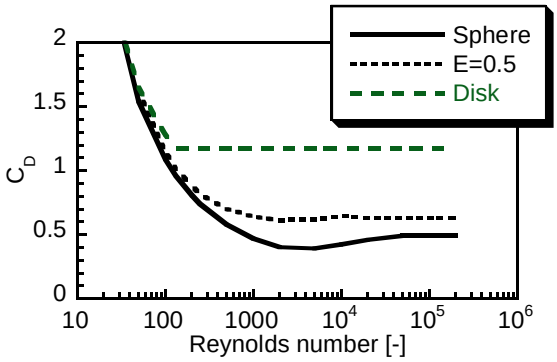

Figure 1: Aerodynamic Drag Coefficients of Sphere, Spheroid and Disk.

Shear Breakup Regime

The shear breakup mechanism is dominant for Weber numbers ranging from 80-800 [10]. After the initial deformation phase, the drop disintegration process includes an extensive system of ligaments protruding from the periphery of the parent drop, with numerous individual drops near the downstream end of the ligaments. It has been observed that drop sizes mainly depend on the viscosity rather than on the surface tension of the liquid phase [10]. A boundary layer stripping approach has been adopted here to model this breakup mechanism and the results show very good agreement with observations from isolated drops in shock tubes.

The rate of disintegration is found by integrating over the thickness of the liquid boundary layer to determine the mass flux in the layer and by assuming that this flux leaves the surface of the drop at its equator [11]. A steady-state solution for the velocity profile is sought, both in the air stream and inside the drop, assuming axisymmetric, incompressible flow. Based on these assumptions, the boundary layer momentum integral equations for the gas are:

$$\frac{\partial}{\partial x}\int_0^\infty u_G(U-u_G)dy + \frac{dU}{dx}\int_0^\infty (U-u_G)dy + \\ + \frac{1}{r}\frac{dr}{dx}\int_0^\infty u_G(U-u_G)dy = \nu_G\left(\frac{\partial u_G}{\partial y}\right)_{y=0} \tag{17}$$

and for the liquid:

$$\frac{\partial}{\partial x}\int_0^\infty u_L^2 dy + \frac{1}{r}\frac{dr}{dx}\int_0^\infty u_L^2 dy = \\ = -\nu_L\left(\frac{\partial u_L}{\partial y}\right)_{y=0} - \frac{1}{\rho_L}\frac{dp}{dx}\delta_L \tag{18}$$

Equating the shear stress in the gas layer to that in the liquid layer at the interface, yields a third equation:

$$-\mu_L\left(\frac{\partial u_L}{\partial y}\right)_{y=0} = \mu_G\left(\frac{\partial u_G}{\partial y}\right)_{y=0}. \tag{19}$$

The velocity distributions in the liquid and gas phases can be derived using Blasius series analysis [12-14], but this method results in a system of differential equations. Assuming that the drop shape is similar to that of a sphere, it can be shown that at the equator,

$$a_L = \sqrt{\frac{8}{3}\frac{\nu_L}{AU_\infty}},\quad A=\left(\frac{\rho_G}{\rho_L}\right)^{2/3}\left(\frac{\nu_G}{\nu_L}\right)^{1/3}. \tag{20}$$

The mass of fluid in the circumferential liquid layer being swept along by the gas stream at a distance $x=\pi D/4$ from the stagnation point is:

$$\frac{dm}{dt} = \pi D\rho_L\int_0^\infty u_L dy = \frac{3}{4}(\pi D)^{3/2}\rho_L A a_L U_\infty, \tag{21}$$

where U_∞ is the relative velocity of the drop.

The boundary layer stripping mechanism has been evaluated by comparing the mass stripping rate with the correlation given by Chou et al. [10]:

$$\dot{m}_p = 0.42\frac{\pi\rho_L d_o^3}{6t^*}e^{\left[0.8\left(t/t^*-3.5\right)^2\right]},\quad 1.5\le t/t^*\le 5.5. \tag{22}$$

The correlation provides the mass rate of formation of dispersed drops due to boundary layer stripping and according to Chou et al. it provides a reasonably good fit for the rate of removal of drop liquid from the parent drop, except for the singular points at the beginning and end of the period where drop mass is being removed. In Figure 2 the comparison between the two methods is shown. The conditions used for this comparison include

an initial droplet size of 20μm, velocity of 200m/s, ambient pressure of 15bar and surface tension of 0.02N/m, which results in a Weber number of 600. The comparison shows very good agreement with the correlation for $2.5<t/t^*<4.5$. The dimensionless time here refers to the time from the beginning of the secondary atomization process. It is interesting to note that experimental measurements were available only for this time period and the correlation has been developed based on that. The initial conditions of the problem (such as velocity, drop diameter and ambient pressure) have been varied and a wide range of Weber numbers have been tested. The agreement is excellent both for the shear breakup regime (80<We<800), for which the correlation has been originally developed, as well as for the catastrophic breakup regime (800<We), as explained in the following section.

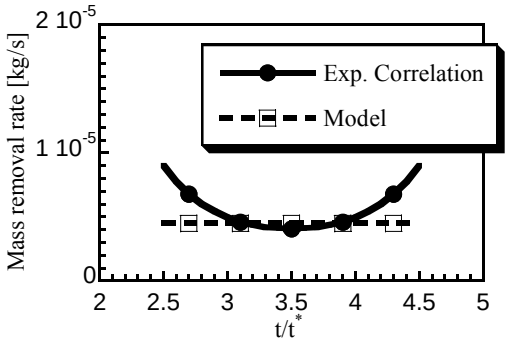

Figure 2: Comparison of Boundary Layer Stripping model (eq. 21) with experimental correlation (eq. 22 [10]), We=600.

Catastrophic Breakup Regime

The catastrophic breakup mechanism is typically observed for Weber numbers larger than 800 and has certain similarities with the shear breakup mechanism. A boundary layer stripping mechanism is present, combined with large waves on the surface of the drop. The growth of instability coupled with the drop deformation into a thin disk is sufficient to shatter the parent drop into a cloud of fragments, which are still large compared to the boundary layer thickness. The resulting fragments further disintegrate through the boundary layer stripping mechanism, thus accelerating the drop disintegration into a fine mist of small droplets. These two mechanisms were studied experimentally by Ranger and Nicholls [11, 14].

A mechanism for fragmenting the liquid drop is evident in the instability of the drop windward surface that is observed as early as $t^*=0.4$. Imbalance between applied pressure, inertia and surface tension effects results into instability of the accelerating interface. Wavelengths of these disturbances are large compared to the boundary layer thickness, so their growth is not significantly influenced by the existence of the boundary layer. An instability analysis based on the work done by Fishburn will be presented here to model the drop fragmentation process [13]. The process of drop fragmentation combined with the boundary layer stripping mechanism is schematically shown in Figure 3. This approach is different from the KHRT model proposed by Patterson and Reitz [3], who only consider two different instability mechanisms and the fastest one is selected to model the drop atomization, but do not take into account the stripping from the drop boundaries.

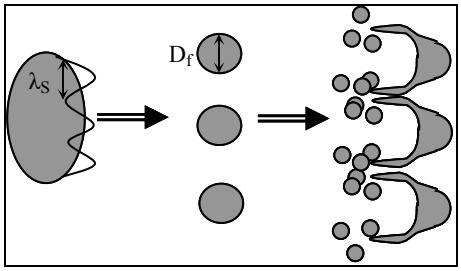

Figure 3: Catastrophic breakup concept

The initial growth rate of a small amplitude sinusoidal disturbance on an accelerating gas-liquid interface is given as [16]:

$$\eta = \eta_o \exp\left(kG - k^3 \frac{\sigma}{\rho_L} \right)^{1/2} t , \qquad (23)$$

where G is the surface acceleration and k the wavenumber. The surface acceleration can be estimated as:

$$G = 2.2 \frac{\rho_G}{\rho_L} \frac{u_G^2}{D_o} . \qquad (24)$$

The wavenumber $k=k_S$ maximizing the expression

$$kG - k^3 \frac{\sigma}{\rho_L} \qquad (25)$$

is used to calculate the wavelength, $\lambda_S=2\pi/k_S$. The initial amplitude of the disturbance, η_o, is given by:

$$\eta_o = \sqrt{\frac{\nu_L D_o}{2u}} \qquad (26)$$

The dimensionless time, t/t^*, required for a bubble to penetrate into the liquid drop is assumed to be equal to the drop fragmentation time and is determined from:

$$D_o = \frac{3}{2}\left\{0.2\lambda + 0.33\sqrt{G\lambda}\cdot B\right\}(1+bt)^2,$$
$$B = \left[\frac{D_o}{u_G}\sqrt{\frac{\rho_L}{\rho_G}}t^* - \frac{\ln(0.2\lambda/\eta_o)}{\sqrt{kG - k^3\sigma/\rho_L}}\right] \quad (27)$$

if the difference in the square brackets is positive, otherwise:

$$D_o = \frac{2}{3}\eta_o \exp\left[\sqrt{kG - k^3\sigma/\rho_L}\,\frac{D_o}{u_G}\sqrt{\frac{\rho_L}{\rho_G}}t^*\right](1+bt)^2 \quad (28)$$

where b=1.6, based on [11]. The diameter of the resulting drop fragments, D_f, is assumed to be equal to the wavelength λ_S. Drop fragments created with this mechanism are subject to boundary layer stripping, as described in the previous section, thus accelerating the disintegration process.

Evaluation of Computational Models

The experimental data of Habchi et al. [17] have been used to evaluate the model and compare against diesel spray measurements. Their experimental apparatus consists of a high-pressure, high-temperature, constant volume cell. The injector used is a common rail unit with electronic control that can supply fuel pressure of 20-150 MPa. The injector was fitted with a single-hole tip with the hole on the axis of the injector. Spray penetrations for three different injection pressures were measured with a Mie scattering technique. In Figure 4 a comparison of spray tip penetration for injection pressures of 40, 80 and 150 MPa is shown, with very good agreement with experimental measurements. The ambient pressure was set to 3 MPa and the temperature to 400K. The model was initialized by injecting blobs with diameter equal to the nozzle diameter (200μm), in order to represent the liquid core of the spray. The constant k_1, controlling the primary breakup rate, was set to 0.5 in order to obtain an atomization rate that results in spray tip penetration in agreement with the experimental measurements. This value has been held constant throughout the injection pressure sweep, showing that the tip penetration scales with injection pressure.

Droplet size measurements are not reported in [17]; however, in Figure 5 the average droplet sizes resulting from the primary atomization as well as the average Weber numbers, computed at the beginning of the secondary atomization process, are presented for each one of the three injection pressures. It appears that the average Weber number increases with injection pressure, even though the droplet size does not change significantly; this can be explained from the higher droplet velocity. In Figure 6 the distribution of the initial Weber numbers for the three injection pressure cases is shown. It appears that for injection pressure of 40 and 80 MPa all the drops undergo secondary atomization according to the shear breakup mechanism. As the injection pressure increases to 150 MPa a portion of the drops has We>800 and atomizes according to the catastrophic breakup mechanism. It is expected that the catastrophic breakup regime becomes more important for higher injection and cylinder pressures.

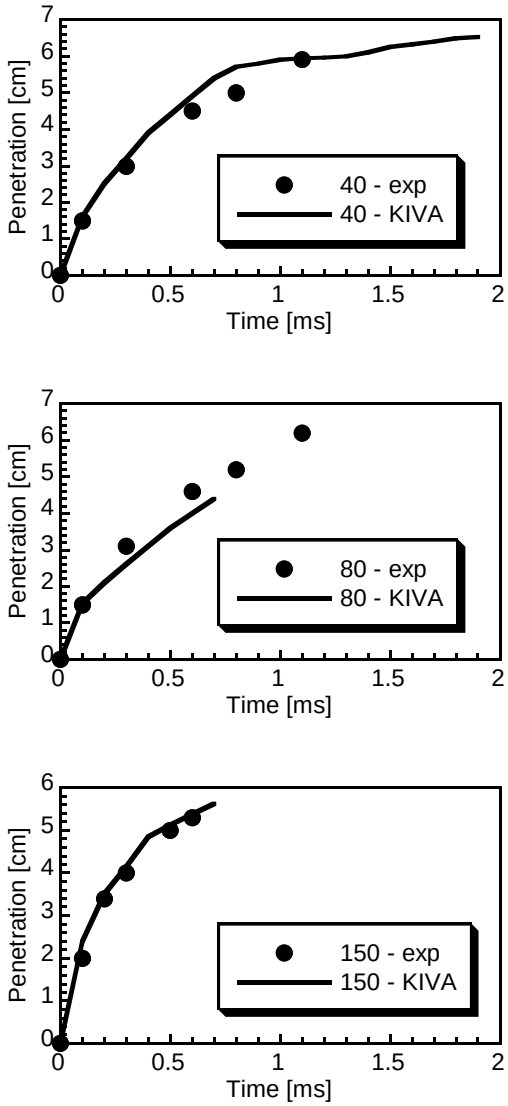

Figure 4: Experimental [17] and CFD-predicted tip penetration for P_{inj}=40, 80, 150 MPa.

Conclusions

A comprehensive model for the primary and secondary atomization of liquid sprays under high injec-

tion pressures has been developed. The primary atomization modeling is based on previous work by Huh et al. [6], assuming a turbulence induced wave growth process resulting in the disintegration of the liquid core. The secondary atomization has been divided in two regimes, namely the shear and the catastrophic breakup regime. In the shear breakup regime a boundary layer stripping model has been used, based on experimental observations of Chou et al. [10]. The catastrophic atomization process is modeled using an instability analysis that leads to drop fragmentation. Subsequently, the resulting fragments disintegrate following the same boundary layer stripping mechanism encountered in shear breakup. A preliminary model validation has been performed by comparing the model predictions with experimental measurements of isolated drops and fully-developed non-evaporating diesel sprays. Further validation is essential in order to demonstrate the capabilities of the model.

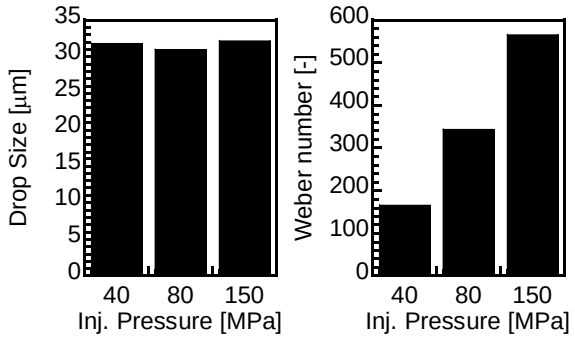

Figure 5: Average Weber number and initial droplet diameter for P_{inj}=40, 80, 150 MPa.

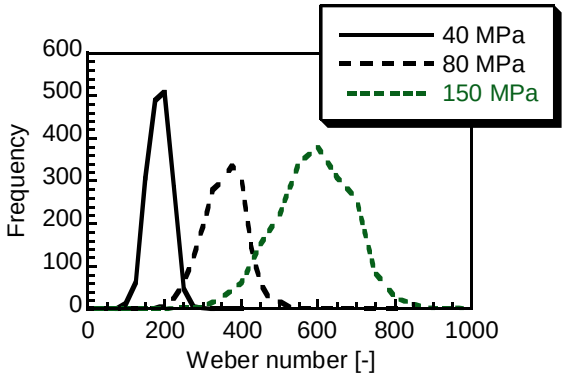

Figure 6: Distribution of Weber number for P_{inj}=40, 80, 150 MPa, CFD predictions.

References

1. Faeth, G.M., Hsiang, L.-P., Wu, P.-K., "Structure and Breakup Properties of Sprays", *Int. J. Multiphase Flow,* Vol. 21, Suppl. pp. 99-127, 1995
2. Reitz, R.D., "Modeling Atomization Processes in High-Pressure Vaporizing Sprays", *Atomization and sprays Technology*, vol. 3, pp. 309-337, 1987
3. Patterson, M.A., Reitz, R.D., "Modeling the Effects of Fuel Spray Characteristics on Diesel Engine Combustion and Emission", SAE 980131, 1998
4. O'Rourke, P.J., Amsden, A.A., "The TAB Method for Numerical Calculation of Spray Droplet Breakup", SAE 872089, 1987
5. Reitz, R.D., Bracco, F.V., "On the Dependence of Spray Angles and Other Spray Parameters on Nozzle Design and Operating Conditions", SAE 790494, 1979
6. Huh, K.Y., Lee, E., Koo, J.-Y., "Diesel Spray Atomization Model Considering Nozzle Exit Turbulence Conditions", *Atomization and Sprays*, vol. 8, pp. 453-469, 1998
7. Hsiang, L.-P., Faeth, G.M., "Near-Limit Drop Deformation and Secondary Breakup", *Int. J. Multiphase Flow*, vol.18, No. 5, pp. 635-652, 1992
8. Aalburg, C., van Leer, B., Faeth, G.M., "Deformation and Drag Properties of Round Drops Subjected to shock Wave Disturbances", *AIAA Journal*, vol. 41, No. 12, December 2003
9. Clift, R., Grace, J.R., Weber, M.E., "Bubbles, Drops and Particles", Academic Press, 1978
10. Chou, W.-H., Hsiang, L.-P., Faeth, G.M., "Temporal properties of drop breakup in the shear breakup regime", *Int. J. Multiphase Flow*, vol. 23, No. 4, pp. 651-669, 1997
11. Ranger, A.A., Nicholls, J.A., "Aerodynamic Shattering of Liquid Drops", *AIAA Journal*, vol. 7, no. 2, pp. 285-290, February 1969
12. Schlichting, H., "Boundary layer theory", 6th ed., McGraw-Hill, 1968
13. Fishburn, B.D., "Boundary layer stripping of liquid drops fragmented by Taylor instability", *Acta Astronautica*, vol. 1, pp. 1267-1284, Pergamon Press, 1974
14. Ranger, A.A., "The Aerodynamic Shattering of Liquid Drops", Ph.D. Dissertation, University of Michigan, Ann Arbor, 1968
15. Taylor, G.I., "The Shape and Acceleration of a Drop in a High Speed Air Stream", The Scientific Papers of G.I. Taylor, edited by G.K. Batchelor, Vol. III, University Press, Campbridge, 1963
16. Taylor, G.I., "The instability of liquid surfaces when accelerated in a direction perpendicular to their planes", Proc. Royal Soc. A. 201, pp. 192-196, 1950
17. Habchi, C., Verhoeven, D., Huynh Huu, C., Lambert, L., Vanhemelryck, J.L., Baritaud, T., "Modeling Atomization and Break Up in High-Pressure Diesel Sprays", SAE 970881, 1997